Effect of Coding in Digital Microcellular Personal Communication Systems with Co-Channel Interference, Fading, Shadowing, and Noise

Jean-Paul M. G. Linnartz, *Member, IEEE,* Aart J. 'T Jong, and Ramjee Prasad, *Senior Member, IEEE*

Abstract—**An analytical model is developed for the performance of a microcellular radio network in the presence of co-channel interference and additive white Gaussian noise. The modulation schemes considered are BPSK, BFSK, and QPSK. The multiple-access channel is statistically modeled by one Rician-distributed desired signal and several uncorrelated Rayleigh plus log-normally shadowed interfering signals, propagating according to dual path loss law with a turning point. The performance is determined in terms of bit error rate (BER), outage probability, block error probability, crosstalk probability, and spectrum efficiency, considering both fast and slow multipath fading. The effect of error correction codes, consisting of blocks with equal number of bits, on the performance parameters is also studied.**

The computational results show that the propagation loss exponents, Rician factor, turning point, and cell size all play a major role in the design of an efficient microcellular system. A proper compromise has to be achieved between spectrum efficiency and bit error rate. The error correction capability of BCH code has a significant effect on the performance for fast multipath fading. However, with slow multipath fading and/or severe shadowing, the effect of error correction is much smaller. Unshadowed fast multipath fading is less harmful than (shadowed or unshadowed) slow multipath fading when appropriate coding is used.

I. Introduction

PERSONAL communication networks (PCN) by radio face two major problems, namely, spectrum scarcity and capacity limitations. To a large extent, both problems can be solved by incorporating a digital microcellular radio system together with the existing macrocellular systems. Microcells, with radius from 0.2 to 2 km, operate at much lower power (less than 20 mW) compared to 0.6–10 W in macrocells with radius typically 2–20 km.

Macrocellular systems have been studied extensively in numerous papers, e.g., [1]–[4], but microcells still need special attention due to their different propagation characteristics. Recently, propagation measurement results for microcells have been reported, e.g., [5]–[9]. Based on these propagation measurement results, performance analysis of microcellular radio systems was carried out in [10]–[12]. The outage probability has been evaluated in [10] without considering the path loss law. A proper path loss law was incorporated in [11], where the co-channel interference probability was computed. The bit error rate (BER) was investigated in [12] for a DPSK modulation scheme. In [10]–[12], the desired signal and co-channel interference were assumed to be Rician (since a direct line-of-sight path exists) and Rayleigh distributed, respectively. However, the propagation measurements show that the co-channel interference also undergoes log-normal shadowing, due to the larger propagation distances from cells at the frequency reuse distance.

In this paper, first the bit error rate is evaluated for Binary Phase Shift Keyed (BPSK), Binary Frequency Shift Keyed (BFSK), and Quadrature Phase Shift Keyed (QPSK) radio signals in the presence of Rayleigh-faded co-channel interference with shadowing as well as additive white Gaussian noise (AWGN). The analysis of the performance of personal communication networks is then extended by considering blocks of bits and introducing different error correction/detection BCH codes [13]. The performance parameters have been evaluated as a function of reuse distance and cluster size of the microcellular network in different propagation scenarios.

This paper is organized as follows. In Sections II and III, respectively, the propagation model and the receiver model are developed. In Section IV, the bit error rate is evaluated. In Section V, error correction/detection codes are introduced; while in Sections VI, VII, and VIII the outage probability, the block error probability, and the probability of erratic receiver capture by a co-channel interferer in another cell (for short, crosstalk probability) are evaluated, respectively. Finally, conclusions are given in Section IX.

II. Propagation Model

In cellular mobile radio, three different and mutually independent propagation phenomena influence the power of the received signal, viz, UHF ground wave path loss, multipath fading, and shadowing. The propagation model adopted in this

Manuscript received March 17, 1992; revised December 15, 1992 and January 27, 1993. This is an expanded version of the work originally presented at the 1st International Conference on Universal Personal Communications, Dallas, TX, September 29–October 2, 1992.

J.-P. M. G. Linnartz was with the Telecommunication and Traffic-Control Systems Group, Delft University of Technology, 2600 GA Delft, The Netherlands. He is now with the University of California, Berkeley, CA 94720.

A. J. 'T Jong and R. Prasad are with the Telecommunication and Traffic-Control Systems Group, Delft University of Technology, 2600 GA Delft, The Netherlands.

IEEE Log Number 9208645.

paper is based on the propagation measurements reported in the literature for the microcellular radio environment [5]–[9].

First, the overall path loss causes the received power to vary gradually, due to signal attenuation determined by the geometry and electromagnetic properties at UHF of the path profile in is entirety. These effects determine the "area-mean" power, denoted as $\bar{\bar{p}}_j$. The received area-mean power $\bar{\bar{p}}_j$ can be described by from the (normalized) propagation law [7], [9]

$$\bar{\bar{p}}_j = c\bar{\bar{p}}_{tx} \frac{r_j^{-a}}{\left(1+\frac{r_j}{g}\right)^b} \tag{1}$$

with $\bar{\bar{p}}_{tx}$ representing the transmitted area-mean power, C a constant, and r_j the propagation distance between transmitter and receiver. The exponent a is the basic propagation loss exponent for short distances, while the exponent b accounts for the additional propagation loss exponent for distances beyond the turning point g of the attenuation curve, between 100 and 200 m.

In this paper, the propagation model for the path loss described in [7], [9], [11], and [12] is used.

Second, in a mobile communication channel, the locally received signal is usually a superposition of a large number of reflected waves. Here, we consider only narrowband channels, i.e., all reflected waves are assumed to add coherently. The received signal is on the form of

$$v_j(t) = (C_j + \zeta_j)\cos\omega_c t + \xi_j \sin\omega_c t \tag{2}$$

where C_j represents the line-of-sight component of the jth signal, i.e., a direct path (without reflections) between transmitter and receiver is assumed to exist. The in-phase and quadrature components of the jth signal, ζ_j and ξ_j, respectively, consist of many reflections and are independent Gaussian distributed random variables with identical probability density functions (pdf's), on the form of $N(0, \sigma_{r,j}^2)$, i.e., with zero mean and variance equal to the local-mean reflected power $\sigma_{r,j}^2$. The instantaneous signal power p_O of the desired signal has the Rician pdf [14]

$$f_{p_O}(p_O|\bar{p}_O) = \frac{1}{\sigma_{r,O}^2} \exp\left(-\frac{2p_O + C_O^2}{2\sigma_{r,O}^2}\right) I_O\left(\frac{\sqrt{2p_O C_O^2}}{\sigma_{r,O}^2}\right) \tag{3}$$

where local-mean power $\bar{p}_O = 1/2C_O^2 + \sigma_{r,O}^2$. In (3), $I_O(\cdot)$ represents the Bessel function of the first kind and zeroth order. On the other hand, the interfering signals arrive from larger distances. Their line-of-sight components are therefore assumed to be negligible, so the instantaneous power of the jth interfering signal p_j, ($p_j = 1/2\rho_j^2 = 1/2\zeta_j^2 + 1/2\xi_j^2$), is exponentially distributed about the local-mean power $\bar{p}_j$, and the amplitude ρ_j has a Rayleigh pdf.

$$f_{p_j}(p_j|\bar{p}_j) = \frac{1}{\bar{p}_j} \exp\left(-\frac{p_j}{\bar{p}_j}\right). \tag{4}$$

Third, the desired signal is unlikely to experience significant shadowing, while interfering signals will in general propagate over obstructed paths because of the larger propagation distances. Accordingly, $\bar{p}_j$ is assumed to be log-normally distributed around the area-mean power $\bar{\bar{p}}_j$, which is determined by a significant path loss. In the corresponding pdf,

$$f_{\bar{p}_j}(\bar{p}_j|\bar{\bar{p}}_j) = \frac{1}{\sqrt{2\pi}\,\sigma_s \bar{p}_j} \exp\left(-\frac{1}{2\sigma_s^2} \ln^2\left(\frac{\bar{p}_j}{\bar{\bar{p}}_j}\right)\right), \tag{5}$$

σ_s represents the logarithmic standard deviation of the shadowing expressed in the absolute values. The standard deviation s_s expressed in decibels is found from $s_s = 4.34\sigma_s$ [11]. The method proposed in [15] is used to estimate the pdf of the joint interference power of several log-normal signals: to a good approximation, the local-mean total interference power caused by the power sum of a number of log-normally distributed signals has also a log-normal distribution. In [2], the logarithmic mean m_n in decibels (with $\bar{p}_j = 10^{m_n/10}$) and standard deviation s_s of the interference power have been determined for a various number of contributing signals.

III. Receiver Model

We consider three types of modulation schemes: BPSK, BFSK, and QPSK. A typical joint receiver input $v(t)$ has the form

$$v(t) = \rho_0 \kappa_0(t)\cos(\omega_c t + \theta_0) + \sum_{j=1}^{n} \rho_j \kappa_j(t)\cos(\omega_c t + \theta_j) + n(t), \tag{6}$$

where $\kappa_j(t)$ ($\kappa_j(t) = \pm 1$) represents the antipodal binary phase modulation of the jth carrier and $n(t)$ is an AWGN process. The received energy per bit is $E_b = p_O T_b = 1/2\rho_O 2T_b$.

In a BPSK detector, $v(t)$ is multiplied by a locally generated cosine ($2\cos\omega_c t$) and integrated over the entire bit duration T_b. The bit clock synchronization offset of the jth interfering signal is denoted as α_j ($0 \le \alpha_j \le 1$). The decision variable ν for synchronous bit extraction from the desired BPSK signal (with index 0) in the presence of n interfering carriers with random (but constant) phase relative to the local oscillator is

$$\begin{aligned}\nu &= \frac{2}{T_b}\int_{kT_b}^{(k+1)T_b} v(t)\cos(\omega_c t)\,dt \\ &= \rho_O \kappa_O(t)\cos(\theta_O) \\ &\quad + \sum_{j=1}^{n} \zeta_j\{\kappa_{j\leftarrow}(kT_b)\alpha_j \\ &\qquad + \kappa_{j\rightarrow}((k+1)T_b)(1-\alpha_j)\} + n_i\end{aligned} \tag{7}$$

with n_j representing the (in-phase) sample of the AWGN. The variance of this noise sample is N_O/T_b (N_O is the noise spectral density). In a Rayleigh-fading channel, all in-phase carrier components ζ_j ($\zeta_j = \rho_j \cos\theta_j$) of the n interferers are mutually independent Gaussian variables, with variance $\bar{p}_j$. The worst interference occurs if the two overlapping interfering bits have identical polarity ($\kappa_j(kT_b) = \kappa_j((k+1)T_b)$). Because the carrier phase of the interfering signal is random within $[0, 2\pi\rangle$, we may confine ourselves to interference with $\kappa_j(kT_b) = \kappa_j((k+1)T_b) = +1$. Considering the possibility

of a phase reversal of the interference yields approximately 1.8 dB lower error rates than pessimistically assuming the worst-case bit sequence for all interfering signals [16]. Here we adopt the worst-case approximation to simplify the analysis and provide conservative results.

The joint interference-plus-noise sample has the distribution $N(0, \overline{p}_t + N_O/T_b)$ with local-mean total co-channel interference power $\overline{p}_t = \Sigma \overline{p}_j$ with $j = 1, \cdots, n$. The conditional BER for a receiver locked to the desired signal is thus

$$P_e(e|p_O, \overline{p}_t) = \frac{1}{2}\operatorname{erfc}\left(\sqrt{\frac{p_O T_b}{A\overline{p}_t T_b + BN_O}}\right) \tag{8}$$

with $A = 1$ and $B = 1$, and $erfc(\cdot)$ represents the complementary error function [17].

In deriving (8), it is assumed that the carrier tracking loop bandwidth is much smaller than the input signal bandwidth, so that tracking errors due to Doppler-shifted interferers can be neglected. Instructive results can be obtained by considering the receiver perfectly locked to the desired signal, but the validation of the analytical results should be the subject of future investigation, e.g., by simulation of a multiuser mobile environment along the lines in [20].

In a synchronous BFSK detector, each interfering signal introduces a Rayleigh phasor (and a corresponding Gaussian in-phase component) in only one of the two branches of the detector, whereas AWGN introduces a Rayleigh phasor in both branches simultaneously. The integrated in-phase signals in the two branches are subtracted and evaluated at the sampling instant. The joint interference sample has the variance $\overline{p}_t$ while the noise has the variance $2N_O/T_b$. This means that the BER for coherent detection of BFSK is again found from (8), but with N_O replaced by $2N_O$, i.e., with $A = 1$ and $B = 2$. In a QPSK transmitter, the source bit stream is split into two slower streams, each with bit rate $1/2r_b$, and transmitted as two BPSK signals in phase quadrature. Thus, the BER is again on the form of (8), but now with $A = 2$ and $B = 1$.

IV. Basic Performance Analysis

First, two basic performance characteristics of a microcellular system are analyzed: 1) bit error rate and 2) spectrum efficiency. The bit error rate is derived for BPSK, BFSK, and QPSK modulation without coding.

A. Basic Relations

The normalized reuse distance R_u is defined as the ratio of the distance D between the centers of the nearest neighboring co-channel cells and the cell radius R, i.e., $R_u \triangleq D/R$. The reuse distance and the number of cells per cluster C are related by $R_u = (3C)^{1/2}$. Using (5), a variable y can be defined as

$$y^2 \triangleq \frac{1}{2\sigma_s^2}\ln^2\left(\frac{\overline{p}_t}{\overline{\overline{p}}_t}\right), \quad \text{thus,} \quad \overline{p}_t = \overline{\overline{p}}_t \exp\left(\sqrt{2}\, y\sigma_s\right). \tag{9}$$

Using (1) and (9), the reciprocal of the local-mean total received signal to interference-plus-noise ratio $\overline{\gamma}$ at the receiver is given by

$$\frac{1}{\overline{\gamma}} = \frac{A\overline{p}_t + BN_O/T_b}{(K+1)\sigma_{r,O}^2} = 10^{\frac{m_n}{10}} A R_u^{-a}\left(\frac{1+\frac{R}{g}}{1+\frac{R_u R}{g}}\right)^b \cdot \exp\left(\sqrt{2}\, y\sigma_{s,n}\right) + \frac{BN_O/T_b}{\sigma_{r,O}^2(K+1)} \tag{10}$$

where $\sigma_{r,O}^2(K+1)/(N_O/T_b)$ represents the local-mean signal-to-noise ratio, m_n and $\sigma_{s,n}$ represent the logarithmic mean and logarithmic standard deviation, respectively, of the area-mean power of n interfacing signals, and the Rician factor $K \triangleq C_O^2/2\sigma_{r,O}^2$. To arrive at the (reciprocal of the) area-mean signal-to-interference ratio $\overline{\overline{\gamma}}$, (10) has to be averaged over all possible values of y. If $\sigma_s = 0$, equation (10) simplifies to the model without shadowing in [11], and [12].

B. Bit Error Rate

Using the method described in [2], the area-mean bit error rate can be defined as

$$P_b \triangleq \sum_{i=0}^{n} P_n(e|n) F_n(n) \tag{11}$$

where $F_n(n)$ is the probability of n active co-channel interferers, and the corresponding conditional error rate is given by

$$P_n(e|n) = \int_{-\infty}^{\infty}\int_{0}^{\infty} P_e(\gamma) f_\gamma(\gamma) f_y(y)\, d\gamma\, dy \tag{12}$$

where $\gamma \triangleq p_O/A(\overline{\overline{p}}_t \exp\left(\sqrt{2}\, y\sigma_s\right) + BN_O/T_b$ represents the instantaneous signal-to-interference-plus-noise ratio. The conditional bit error rate $P_e(\gamma)$ for a desired signal is given by (8), where the constants (A, B) equal $(1, 1)$ for BPSK, $(1, 2)$ for BFSK and $(2, 1)$ for QPSK.

Only interfering signals arriving from the nearest neighboring six co-channel cells are considered. The blocking probability B_E, determined by the Erlang-B formula [1], [2], and the number of channels n_c are assumed the same in all cells. The probability of n active co-channel cells is

$$F_n(n) = \binom{6}{n} a_c^n (1 - a_c)^{6-n} \tag{13}$$

where $a_c = A_c/n_c$. The carried traffic can be obtained by $A_c \triangleq A_E(1 - B_E)$, with A_E the offered traffic per cell, in erlang.

For a receiver locked to the desired signal, (3), (5), (9), (10), and (12) give

$$P_n(e|n) = \frac{1}{\sqrt{\pi}}\int_{-\infty}^{\infty}\int_{0}^{\infty} \frac{1}{2}\operatorname{erfc}(\sqrt{\gamma})\, \frac{(K+1)}{\overline{\gamma}} \cdot \exp\left(-y^2 - \frac{\gamma(K+1)}{\overline{\gamma}} - K\right) \cdot I_O\left(\sqrt{\frac{4\gamma K(K+1)}{\overline{\gamma}}}\right) d\gamma\, dy. \tag{14}$$

In the special case that the desired signal suffers from Rayleigh fading (i.e., the line-of-sight component is negligible) and the

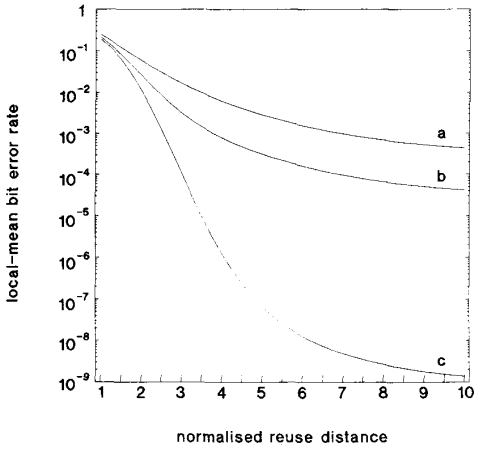

Fig. 1. Local-mean BER with BPSK modulation as a function of the normalized reuse distance R_u with local-mean signal-to-noise ratio $\overline{p}_O/(N_O/T_b) = 30$ dB, $A_c = 5$ erlang, $n_c = 10$ channels per cell, and $G = g/R = 0.67$ for (a) $K = 0$, (b) $K = 6$ dB, and (c) $K = 12$ dB.

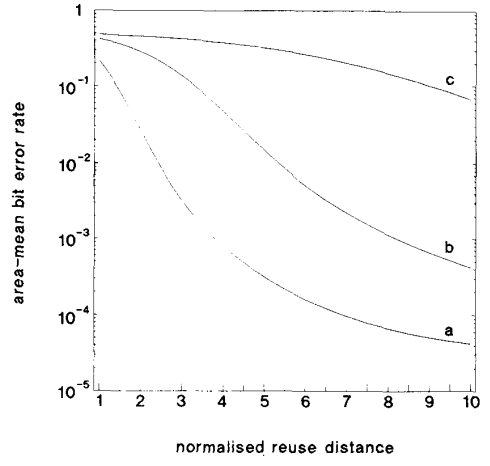

Fig. 2. Area-mean BER with BPSK modulation as a function of the normalized reuse distance R_u with $K = 6$ dB, $A_c = 5$ erlang, $n_c = 10$ channels per cell, and $G = 0.67$ for shadowing of (a) $s_s = 0$ dB, (b) $s_s = 6$ dB, and (c) $s_s = 12$ dB.

interfering signals have no shadow attenuation, a well-known closed-form expression is recovered [14]

$$P_n(e|n) = \frac{1}{2} - \frac{1}{2}\sqrt{\frac{\overline{\gamma}}{\overline{\gamma}+1}} \tag{15}$$

where $\overline{\gamma}$ is given by (10) for $K = 0$ and $\sigma_s = 0$.

In Fig. 1, the local-mean BER with BPSK modulation is plotted as a function of the normalized reuse distance R_u, with Rician factor K as a parameter. A higher value of K offers a better performance. In macrocellular systems, where both the desired signal and co-channel interferers are Rayleigh faded, $K = O$.

Fig. 2 shows the area-mean BER with BPSK modulation as a function of R_u, with the standard deviation of the shadowing s_s as a parameter. For increasing values of s_s, the performance deteriorates. The value of $s_s = 0$ dB corresponds to the case of no shadowing.

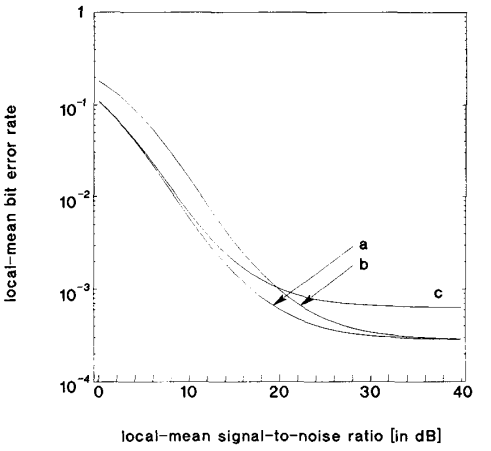

Fig. 3. Local-mean BER with (a) BPSK, (b) BFSK, and (c) QPSK modulation as a function of the local-mean signal-to-noise ratio for $K = 6$ dB, $A_c = 5$ erlang, $n_c = 10$ channels per cell, $G = 0.67$, and $R_u = 5$.

Fig. 3 depicts the local-mean BER with BPSK, BFSK, and QPSK modulation as a function of local mean signal-to-noise ratio. For small values of local-mean signal-to-noise ratio $[\overline{p}/(N_O/T_b)]$ BPSK and QPSK offer a better performance than BFSK, while for higher values of $\overline{p}_O/(N_O/T_b)$ BPSK and BFSK offer a better performance than QPSK. For small values of $\overline{p}_O/(N_O/T_b)$, the effect of AWGN on the BER is much greater than the effect of co-channel interference, while for higher values of $\overline{p}_O/(N_O/T_b)$, co-channel interference becomes more important than AWGN. These results agree with [16], where it was concluded that BPSK and QPSK are 3 dB more resistant against AWGN than BFSK, while BPSK and BFSK are equally resistant against co-channel interference and 3 dB more robust than QPSK. Fig. 4 shows the local-mean BER with BPSK modulation as a function of R_u, with the propagation loss exponents a and b as parameters. In [9], field measurements in several urban areas resulted in different values for a and b. From Fig. 4, it can be seen that a and b have a large effect on the performance. In Fig. 5, the local-mean BER with BPSK modulation is plotted as a function of R_u, with G as a parameter. For a given local-mean signal-to-interference ratio, the BER decreases with a decrease in G $(= g/R)$. Therefore, the radius of the microcell and the turning point play important roles in system design.

C. Spectrum Efficiency

In [11], spectrum efficiency E_s was defined as the carried traffic per cell A_c divided by the product of bandwidth per channel W, the number of channels per cell n_c and the cluster size C cells, given a unit cell area of S_u, i.e.,

$$E_s \triangleq \frac{A_c}{n_c W C S_u} \text{ [erlang/MHz/km}^2\text{]}. \tag{16}$$

With $R_u = (3C)^{1/2}$ and (16), it is possible to express the reciprocal of the local-mean total received signal to interference-plus-noise ratio (10) in terms of the cluster size and spectrum efficiency. In this way, it is possible to investigate also the

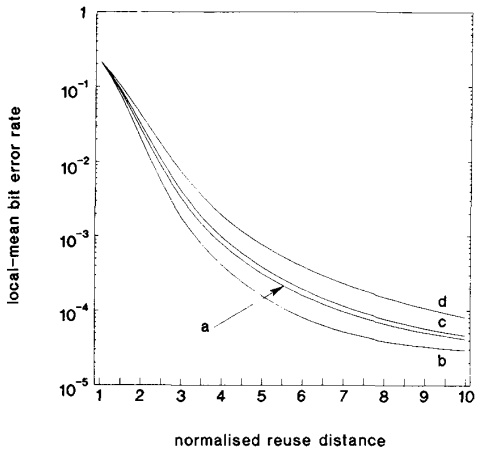

Fig. 4. Local-mean BER with BPSK modulation as a function of the normalized reuse distance R_u with $K = 6$ dB, $A_c = 5$ erlang, $n_c = 10$ channels per cell, and $G = 0.67$ for several attenuation rate coefficients (a) $a = 2, b = 2$; (b) $a = 1.3, b = 3.5$; (c) $a = 1.5, b = 2.5$; and (d) $a = 1.5, b = 3.5$.

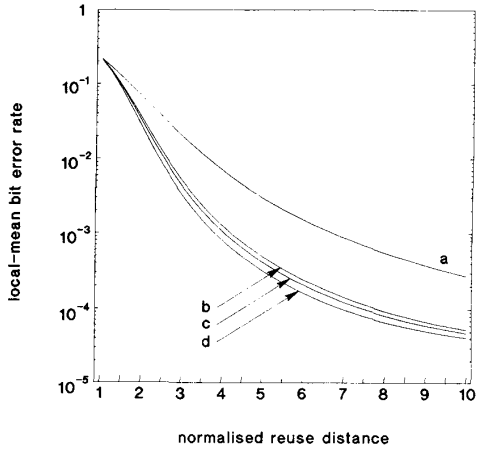

Fig. 5. Local-mean BER with BPSK modulation as a function of the normalized reuse distance R_u with $K = 6$ dB, $A_c = 5$ erlang, $n_c = 10$ channels per cell for (a) $G = 10$, (b) $G = 1.25$, (c) $G = 1$, and (d) $G = 0.67$.

influence of cluster size and spectrum efficiency on the BER (and later on the other performance parameters).

Fig. 6 shows the area-mean BER with BPSK modulation as a function of the spectrum efficiency E_s for several values of s_s. As in Fig. 2, the very significant shadowing effect of s_s on the performance can be seen. For a given BER, higher values of s_s offer a lower spectrum efficiency. It can also be seen that a tradeoff can be made between spectrum efficiency and low BER.

V. Impact of Error Correction/Detection Coding

In the previous section, the bit error rate has been derived, assuming frequency nonselective fading (i.e., $T_b \gg T_m$ [14], with T_m representing the delay spread of desired and cochannel interference, so intersymbol interference is assumed negligible) and slow compared to the bit duration T_b (the

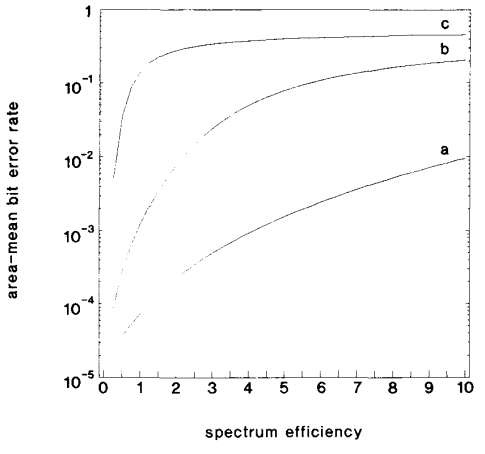

Fig. 6. Area-mean BER with BPSK modulation as a function of the spectrum efficiency SE with $K = 6$ dB, $A_c = 5$ erlang, $n_c = 10$ channels per cell, $G = 0.67$, $W = 25$ kHz, and $S_u = 1$ km^2 for shadowing of (a) $s_s = 0$ dB, (b) $s_s = 6$ dB, and (c) $s_s = 12$ dB.

amplitudes of desired and interfering signals remain constant during one bit). In this section, we are extending the performance analysis of microcellular radio systems to blocks consisting of L bits. We therefore distinguish two extreme types of multipath fading [3], viz. the following:

1) Fast multipath fading (without shadowing): for this case, the bit errors in successive bits are assumed independent and have equal bit error rate for a given local-mean power of the desired signal.

2) Slow multipath fading: for this case, the mobile terminal is assumed to move very slowly so that the signal-to-noise ratio and the signal-to-interference ratio for all L bits within a block or codeword are the same.

The influence of error correction/detection coding is also included. Digital systems employing error correction/detection coding are generally based on the transmission of blocks of L sequential bits, where each codeword of L bits is a voice or data segment. The performance of such systems depends upon the probability of occurrence of errors in a received block. A large variety of error correction\detection codes is known; in this paper, Bose–Chaudhuri–Hocquenghem (BCH) codes with parameters (L, k, t) [13] are considered. L represents the length of the block, k is the number of actual data ("user") bits in a block, and t is the error correction capability, i.e., up to t bits of the block can be corrected. Another code parameter is l, the error detection capability. A code with error detection capability l can detect up to l error bits in a block. With a Hamming distance $d_{\min} \geq 2t + l + 1$, it is possible to trade between error-correction and error-detection capabilities. With a block length L, 2^L possible combinations of bits can be made, but only $M = 2^k$ of these combinations are used as codewords.

A cellular net is assumed with each cell having one transmitter and one mobile terminal, so all possible codewords are assigned to the communication links between transmitter and receiver in all cells. In this way, the same set of codewords is used for each cell. In [3], it was assumed that the receiver is

either successful (i.e., the received block lies within distance t of the transmitted codeword) or unsuccessful. An "*outage*" can then be defined as the event that the received block does not lie within distance t of the transmitted codeword. In [4], the events when the receiver is unsuccessful (i.e., an outage) are divided into two parts, viz. "*failures*" (the received block does not lie within distance t of any codeword), and *errors* (the received block does not lie within distance t of a codeword, however, that codeword has not been transmitted by the transmitter in the "home" cell). Errors consist partly of random errors and partly of "*crosstalks*". A cosstalk is the event that a codeword is decoded at the receiver in the home cell, while this codeword has been transmitted by a transmitter in one of the co-channel cells. This event is likely to occur when one of the interfering signals happens to dominate the desired signal and all other interfering signals. In this way, a data or voice segment is decoded that is not destined for the receiver considered. This event is highly undesirable, particularly since it may continue for several successive blocks.

In the following sections, expressions for the outage probability, the block error probability, and the crosstalk probability are derived. From this point on, continuous transmission of radio signals between transmitter and receiver in all cells is assumed. This means that $F_n(n) = 1$, so (12) is then equal to (11).

VI. Outage Probability

Section IV presented the bit error probability and spectrum efficiency without considering error correction/detection coding. In the previous section, the outage probability with coding was defined as the probability that the received block does not lie within distance t of the codeword that was transmitted by the transmitter in the home cell. When bit errors occur independently, the conditional probability of m errors in a block of L bits can be given as [18]

$$P_{block}(m \text{ errors}|\gamma) = \binom{L}{m}(P_e(e|\gamma))^m(1 - P_e(e|\gamma))^{L-m} \tag{17}$$

where $P_e(e|\gamma)$ represents the bit error rate (8) for a given instantaneous signal-to-interference-plus-noise ratio. With (17), the expression for the outage probability can be given as

$$P_{block}(\text{outage}|\gamma) = 1 - \sum_{m=0}^{t}\binom{L}{m}(P_e(e|\gamma))^m \cdot (1 - P_e(e|\gamma))^{L-m}. \tag{18}$$

Assuming fast multipath fading, the local-mean outage probability can be found by substituting the local-mean BER (given by (14) with $\sigma_s = 0$) instead of the instantaneous BER (8) into (18). Because shadowing is assumed to be slow compared to the duration of a codeword, the area-mean outage probability can be found by averaging the local-mean outage probability over the shadowing. Assuming slow multipath fading, the local-mean outage probability can be found by averaging (18) over the pdf of the multipath fading given by (3). The are-mean outage probability can be found by averaging the local-mean outage probability over the shadowing.

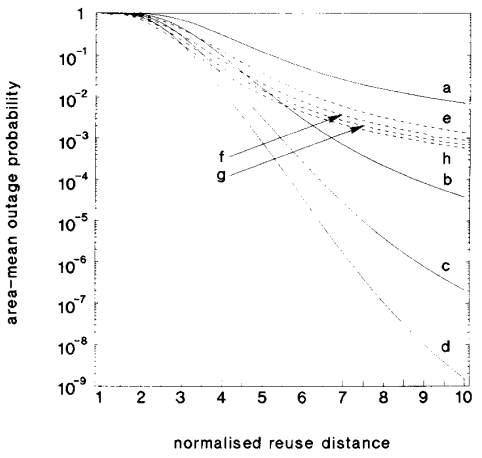

Fig. 7. Area-mean outage probability for BPSK modulation as a function of the normalized reuse distance R_u with $K = 6$ dB and $G = 0.67$ for error correction capability $t = 0, 1, 2, 3$ for (—, a–d, respectively) fast and (- -, e–h, respectively) slow multipath fading.

Numerical results for the outage probability are given by Figs. 7 and 8. Linear BCH block codes with a block length $L = 63$ bits are used. Fig. 7 shows the area-mean outage probability with BPSK modulation as a function of R_u, for both fast and slow multipath fading, with error correction capability t as a parameter. The major effect of t on the performance with fast multipath fading can be seen; this effect is almost negligible with slow multipath fading. Thus, except in the absence of coding (i.e., with $t = 0$), the performance in fast multipath fading is better than in slow multipath fading. The difference can be explained by the fade duration. The duration of the fast fades is small compared to the duration of a block (codeword) LT_b. Therefore, it is likely that only a few bits of the transmitted codeword are received incorrectly. With error correction capability t, up to t bits erroneous bits can be corrected, and so most received blocks will decoded correctly. On the other hand, the duration of the slow fades is of the same order as (or greater than) the duration of a block. Therefore, the effect of higher values of t is very small. In Fig. 8, the area-mean outage probability with BPSK modulation is plotted as a function of R_u, for fast and slow multipath fading, with s_s as a parameter. Again, the standard deviation of the shadowing plays an important role in determining the performance. For $s_s = 12$ dB, fast multipath fading, and small values of R_u, the performance is even worse than the performance assuming slow multipath fading. This phenomenon can also be explained by the fade duration, which is even longer with shadowing than for slow multipath fading, so error correction is less useful than in the event of slow multipath fading without shadowing.

VII. Block Error Probability

The block error probability is now derived based on the geometric considerations presented in [4]. The number of blocks v_t and v_{t+l} that lie within a distance t and within a distance $t+l$ or less from a codeword, respectively, are called

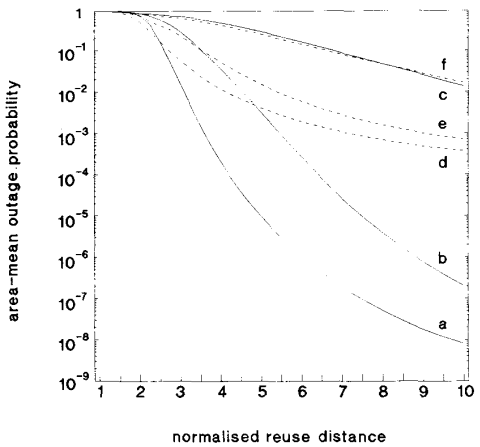

Fig. 8. Area-mean outage probability for BPSK modulation as a function of the normalized reuse distance R_u with $K = 6$ dB and $G = 0.67$ for shadowing of $s_s = 0$ dB, $s_s = 6$ dB, and $s_s = 12$ dB for (—, a–c, respectively) fast and (- -, d–f, respectively) slow multipath fading.

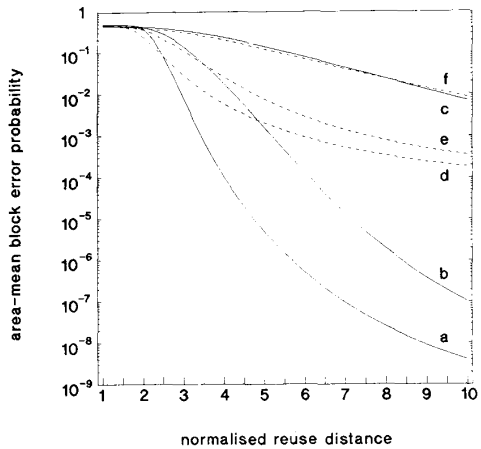

Fig. 9. Area-mean block error probability for BPSK modulation as a function of the normalized reuse distance R_u with $K = 6$ dB and $G = 0.67$ for shadowing of $s_s = 0$ dB, $s_s = 6$ dB, and $s_s = 12$ dB for (—, a–c, respectively) fast and (- -, d–f, respectively) slow multipath fading.

the Hamming spheres with radius t and $t + l$, with

$$v_y = \sum_{m=0}^{t} \binom{L}{m} \quad \text{and} \quad v_{t+l} = \sum_{m=0}^{t+l} \binom{L}{m}. \tag{19}$$

If more than $t + l$ bit errors occur in the received block, the block can be treated as if it were completely random [19]. In that case, the block may lie anywhere in the Hamming space, i.e., any of the $2^L - v_{t+l}$ remaining blocks is assumed equally probable. Thus, the number of possible received blocks left is $2^L - v_{t+l}$, but only $(M-1)v_t$ of these result in an error. The block error probability can be given by

$$\begin{aligned} P_{block}(\text{error}|\gamma) &= \frac{(M-1)v_t}{2^L - v_{t+1}} \\ &\quad \cdot \left(1 - \text{Prob}\left\{\begin{array}{l}\text{received block lies}\\ \text{within distance } t+1\\ \text{of a codeword}\end{array}\right\}\right) \\ &= \frac{(M-1)v_t}{2^L - v_{t+1}} \\ &\quad \cdot \left(1 - \sum_{m=0}^{t+1} \binom{L}{m} (P_e(e|\gamma))^m \right. \\ &\quad \left. \cdot (1 - P_e(e|\gamma))^{L-m}\right). \end{aligned} \tag{20}$$

The local-mean block error probability assuming fast multipath fading can be found by substituting directly the local-mean BER (given by (14) with $\sigma_s = 0$) instead of (8) in (20). Where assuming slow multipath fading, the block error probability has to be averaged over the Rician pdf (3). In either case, the area-mean block error probability can be found by averaging the local-mean block error probability over the shadowing.

The resulting block error probability is shown in Figs. 9 and 10. In Fig. 9, the area-mean block error probability with BPSK modulation is given as a function of R_u, for fast and slow multipath fading, with s_s as a parameter. Fig. 10 shows the area-mean block error probability with BPSK modulation as a function of R_u, for fast and slow multipath fading, with t and l as a parameter, and $k = 51$ user bits. The tradeoff between error correction and error detection is clear from Fig. 10. The block error probability for large l and small t is smaller than the block error probability for large t and small l. This can be explained by the fact that for large values of l (and small t), outages are more often failures than errors.

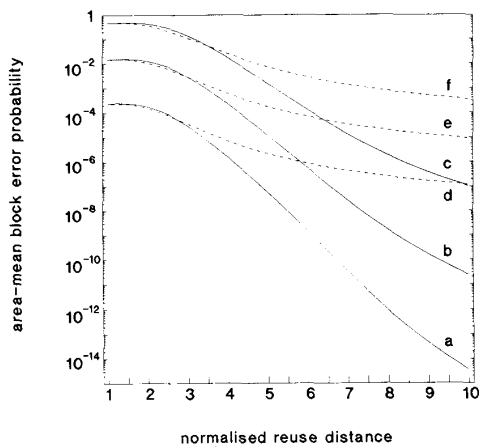

Fig. 10. Area-mean block error probability for BPSK modulation as a function of the normalized reuse distance R_u with $K = 6$ dB, $s_s = 6$ dB, $G = 0.67$, and $k = 51$ bits, for $t = 0$ and $l = 4$, $t = 1$ and $l = 2$, and $t = 2$ and $l = 0$, for (—, a–c, respectively) fast and (- -, d–f, respectively) slow multipath fading.

VIII. Crosstalk Probability

So far, the desired signal was supposed to come from the home cell, and the interfering signals were assumed to arrive from more distant co-channel cells. This changes in the case of crosstalk. In this case, the dominating signal (capturing the receiver instead of the desired signal) is originating from one of the co-channel cells, and a total of six interfering signals

come from five remaining co-channel cells plus the "desired" signal from the home cell.

As was discussed in Section V, a crosstalk occurs if one of the interfering signals dominates the desired signal and the other interfering signals, and causes the received block to lie within distance t of one of the codewords, although this codeword was transmitted by the transmitter in the co-channel cell. Note that if, due to this effect, the received block still lies within distance t of the codeword that was also transmitted by the transmitter in the home cell, a success occurs instead of a crosstalk. Because crosstalks are part of the errors, only $(M-1)v_t/2^L - v_{t+l}$ of the possible received blocks contribute to the crosstalk probability. Because the received block has to lie within distance t of a codeword, the crosstalk probability can be calculated as a success with the capturing signal arriving from distance D (the co-channel cell), and the total interference arriving from distance R and distance D (the home cell and the other five co-channel cells). The local-mean power of the original desired signal $\overline{p}_O$ was given in Section II. A Rician-faded signal is approximated by a $(K+1)$ times stronger Rayleigh-fading signal, thus, the local-mean power of the Rician-faded signal is now expressed as $\overline{p}_O = \overline{p}_{O,Rayleigh}(1+K)$, where $\overline{p}_{O,Rayleigh}$ denotes the local-mean power of the corresponding Rayleigh-faded signal.

As in Section IV, the reciprocal of the local-mean ratio of the received capturing signal power and the total "interfering"-plus-noise power can be obtained, after using (10)

$$\begin{aligned}\frac{1}{\overline{\overline{\gamma}}'} &= \frac{5\overline{p}_j + \overline{p}_{O,Rayleigh}(1+K) + N_O/T_b}{\overline{p}_j} \\ &= \frac{10^{\frac{m_5}{10}}\exp\left(\sqrt{2}\,y\sigma_{s,5}\right)}{\exp\left(\sqrt{2}\,y\sigma_{s,1}\right)} + \frac{R_u^2(K+1)}{\exp\left(\sqrt{2}\,y\sigma_{s,1}\right)}\left(\frac{1+\frac{R_uR}{g}}{1\frac{R}{g}}\right)^2 \\ &\quad + \frac{N_O/T_b}{\exp\left(\sqrt{2}\,y\sigma_{s,1}\right)}(R_uR)^2\left(1+\frac{R_uR}{g}\right)^2 \end{aligned} \tag{21}$$

with $\overline{p}_j$ representing the local-mean power of the single interfering signal, m_5 representing the logarithmic of the total area-mean interference power caused by 5 interfering signals, and $\sigma_{s,1}$ and $\sigma_{s,5}$ representing the logarithmic standard deviations of the shadowing for 1 and 5 interfering signals, respectively. The values for the logarithmic mean and logarithmic standard deviation are calculated according to [2]. To arrive at the reciprocal of the area-mean signal-to-interference ratio $\overline{\overline{\gamma}}'$, (21) has to be averaged over all possible values of y.

In this section, only BPSK modulation is considered. Crosstalks caused by all six co-channel cells have to be taken into account. The probability that the received blocks arriving from the home transmitter and the co-channel transmitter are equal, i.e., $0, 5^L$, is also considered. If the probability of crosstalk is relatively small, then the crosstalk probability can approximately given by

$$\begin{aligned}P_{block}(\text{crosstalk}|\gamma') &\approx 6\,\frac{(M-1)v_t}{2^L - v_{t+1}} \\ &\quad \cdot \left(\text{Prob}\left\{\begin{array}{l}\text{received block lies}\\ \text{within distance } t\\ \text{of a codeword}\end{array}\right\}\right. \\ &\quad \left. - \text{Prob}\left\{\begin{array}{l}\text{received blocks}\\ \text{are equal}\end{array}\right\}\right) \\ &\approx 6\,\frac{(M-1)v_t}{2^L - v_{t+1}} \\ &\quad \cdot \left(\sum_{m=0}^{t}\binom{L}{m}\left\{(P_e(e|\gamma'))^m \right.\right. \\ &\quad \left.\left. \cdot\,(1-P_e(e|\gamma'))^{L-m} - \left(\frac{1}{2}\right)^L\right\}\right)\end{aligned} \tag{22}$$

with $\gamma' = p_j/(5\overline{p}_j + \overline{p}_O + N_O/T_b)$. Here, the approximation that the receiver locks to any interfering signal [21] is used. The local-mean BER can be found by averaging the instantaneous BER for crosstalk $P_e(e|\gamma')$ found from (8), replacing γ by γ', over the Rayleigh pdf (4). Assuming fast multipath fading, the local-mean crosstalk probability can be found by substituting directly the local-mean BER for crosstalk in (22). Assuming slow multipath fading, the local-mean crosstalk probability can be found by averaging the instantaneous probability of crosstalk (22) over the Rayleigh pdf (4). The area-mean crosstalk probability can be found by averaging the local-mean crosstalk probability over the shadowing. It is assumed that the capturing and the other interfering signals arriving from distance D suffer from log-normal shadowing, while the desired signal is unshadowed (as in Section IV).

Results for the crosstalk probability and the block error probability are shown in Figs. 11 and 12 for fast and slow multipath fading, respectively. Both probabilities are given as function of Ru. Shadowing has a major effect on the crosstalk probability, for both fast and slow multipath fading. This can be explained in terms of fade durations. Assuming shadowing, it is more likely that the desired signal becomes smaller than (one of) the interfering signals; this increases the crosstalk probability. Except for severe shadowing ($s_s = 12$ dB), the crosstalk probability remains small compared to the block error probability.

IX. Conclusions

The performance of a digital microcellular radio system has been investigated considering the desired signal as Rician-faded, co-channel interference as Rayleigh faded with log-normal shadowing, and a dual path loss law with a turning point. Results were obtained for BPSK, BFSK, and QPSK modulation, with BCH (L,k,t) error correction coding for a fast and slow frequency nonselective fading channel. For higher values of the Rician factor K, the performance increases, so microcellular systems generally appear to offer better performance than macrocellular systems (for which $K = 0$). The standard deviation s_s of the shadowing has an enormous effect on the performance. Results for the three types of modulation scheme confirm the results found in [16], where it was found that BPSK and BFSK are equally resistant against co-channel interference and 3 dB more robust than QPSK, while BPSK and QPSK are 3 dB more resistant against AWGN than BFSK. The choice of modulation is thus an important

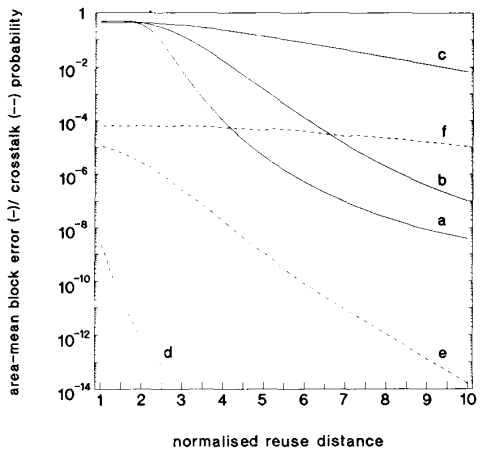

Fig. 11. Area-mean block error probability (—) and crosstalk probability (- -) for BPSK modulation as a function of R_u, with $K = 6$ dB and $G = 0.67$, for fast multipath fading and shadowing of $s_s = 0$ dB (a, d), $s_s = 6$ dB (b, e), and $s_s = 12$ dB (c, f).

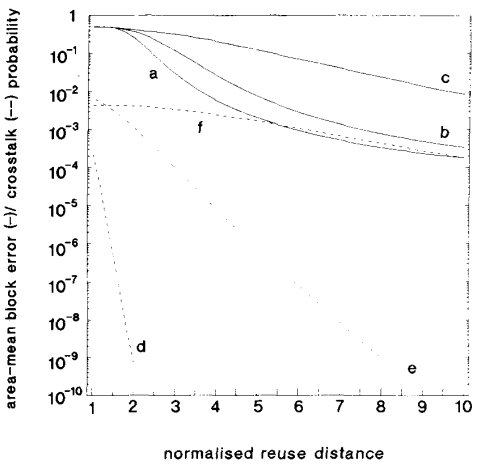

Fig. 12. Area-mean block error probability (—) and crosstalk probability (- -) for BPSK modulation as a function of R_u, with $K = 6$ dB and $G = 0.67$, for slow multipath fading and shadowing of $s_s = 0$ dB (a, d), $s_s = 6$ dB (b, e), and $s_s = 12$ dB (c, f).

design parameter in an interference-limited system. Different values for the propagation loss exponents a and b have been reported in literature and have a substantial effect on the BER. Further, the radius of the microcell relative to the turning point plays an important role in designing the system.

The use of BCH codes has a major effect on the performance in the presence of fast multipath fading, measured in terms of the outage probability, block error probability, and crosstalk probability. The block error probability is also influenced by the error detection capability l of the code used. A tradeoff between error correction and error detection capability can be made. Crosstalks can be reduced, for example, by 1) introducing headers, i.e., use a few bits for an identity code of the transmitter; and 2) use different sets of codewords, separated by a large Hamming distance, in each co-channel cell. Results for the performance show that the effect of coding is much smaller than for fast multipath fading without shadowing. Except for the case that no coding is used, the performance resulting from the analysis assuming fast multipath fading without shadowing is much better than the performance resulting from the analysis assuming slow multipath fading and/or shadowing. Crosstalk becomes important in severe shadowing, while in the absence of shadowing, the crosstalk probability is small.

ACKNOWLEDGMENT

The authors are grateful to Prof. Dr. J. C. Arnbak for review of the paper, and to R. D. J. van Nee for fruitful discussions. They would like to thank the anonymous reviewers for valuable suggestions. The typescript was prepared by E. Ooms and S. Chlimintzas.

REFERENCES

[1] R. Prasad, A. Kegel, and J. C. Arnbak, "Analysis of system performance of high capacity mobile radio," in *Proc. 39th Veh. Technol. Conf.*, San Francisco, CA, May 1989, pp. 306–310.

[2] R. Prasad and A. Kegel, "Improved assessment of interference limits in cellular radio performance," *IEEE Trans. Veh. Technol.*, vol. VT-40, pp. 412–419, May 1991.

[3] I. M. I. Habbab, M. Kavehrad, and C.-E. W. Sundberg, "Aloha with capture over slow and fast fading radio channels with coding and diversity," *IEEE J. Select. Areas Commun.*, vol. SAC-7, pp. 79–88, Jan. 1989.

[4] J. P. M. G. Linnartz and J. J. P. Werry, "Error correction and error detection in a fast fading narrowband slotted Aloha network with BPSK modulation," in *Proc. 1st Int. Symp. Commun. Theory Appl.*, Crieff Hydro Hotel, Scotland, Sept. 9–13, 1991, 7 pp. Paper 37.

[5] R. J. C. Bultitude and G. K. Bedal, "Propagation characteristics on microcellular urban mobile radio channels at 910 MHz," *IEEE J. Select. Areas Commun.*, vol. SAC-7, pp. 31–39, Jan. 1989.

[6] E. Green, "Radio link design for microcellular systems," *Br. Telecom. Technol. 5*, vol. 8, pp. 85–96, Jan. 1990.

[7] P. Harley, "Short distance attenuation measurements at 900 MHz and 1.8 GHz using low antenna heights for microcells," *IEEE J. Select Areas Commun.*, vol. SAC-7, pp. 5–10, Jan. 1989.

[8] S. T. S. Chia, R. Steel, E. Green, and A. Baran, "Propagation and bit error ratio measurements for a microcellular system," *J. Inst. Electric Radio Eng.*, vol. 57, no. 6 (supplement) pp. S255–266, Nov./Dec. 1987.

[9] R. L. Pickholtz, L. B. Milstein, D. L. Schilling, M. Kullback, D. Fishman, and W. H. Biederman, "Field tests designed to demonstrate increased spectral efficiency for personal communications," in *Proc. IEEE Globecom'91*, Phoenix, AZ, 1991, pp. 878–882.

[10] Y.-D. Yao and A. U. H. Sheikh, "Outage probability analysis for microcell mobile radio systems with co-channel interferers in a Rician/Rayleigh fading environment," *Electron. Lett.*, vol. 26, pp. 864–866, June 1990.

[11] R. Prasad, A. Kegel, and J. Olsthoorn, "Spectrum efficiency analysis for microcellular mobile radio systems," *Electron. Lett.*, vol. 27, no. 5, pp. 423–424, 1991.

[12] A. Kegel, H. J. Wesselman, and R. Prasad, "Bit error probability for fading DPSK signals in microcellular land mobile radio systems," *Electron. Lett.*, vol. 27, no. 18, pp. 1647–1648, 1991.

[13] S. Lin and D. J. Costello, Jr., *Error Control Coding—Fundamentals and Applications.* Englewood Cliffs, NJ: Prentice-Hall, 1983.

[14] J. G. Proakis, *Digital Communications*, 2nd ed. (1989). New York: McGraw-Hill, 1983.

[15] S. C. Schwartz and Y. S. Yeh, "On the distribution function and moments of power sums with log-normal components," *Bell Syst. Tech. J.*, vol. 61, no. 7, pp. 1441–1462, Sept. 1982.

[16] J. P. M. G. Linnartz and A. J. 'T Jong, "Average bit error rate for coherent detection in micro and macro cellular radio," in *Proc. 6th IEE Int. Conf. Mobile Radio Personal Commun.*, Warwick, U.K., Dec. 9–12, 1991, pp. 241–247.

[17] M. Abramowitz and I. A. Stegun, *Handbook of Mathematical Functions.* New York: Dover, 1965.

[18] R. E. Eaves and A. H. Levesque, "Probability of block error for very slow Rayleigh fading in Gaussian noise," *IEEE Trans. Commun.*, vol. COM-25, pp. 368–374, Mar. 1977.

[19] R. J. McEliece and L. Swanson, "On the decoder error probability for Reed–Solomon codes," *IEEE Trans. Inform. Theory,* vol. IT-32, pp. 701–703, Sept. 1986.
[20] R. Pluijmers, "Computer simulation of a mobile packet radio system," *Electron. Lett.,* vol. 24, no. 6, pp. 316–317, Mar. 1988.
[21] J. P. M. G. Linnartz, R. Hekmat, and R. J. Venema, "Near-far effects in land-mobile random access networks with narrowband Rayleigh-fading channels," *IEEE Trans. Veh. Technol.,* vol. VT-41, pp. 77–90, Feb. 1992.

Jean-Paul M. G. Linnartz (S'86–M'90) was born in Heerlen, province of Limburg, The Netherlands, on September 10, 1961. He attended Gymnasium β at the Scholengemeenschap St. Michiel in Geleen.

He received the Ir. (M.Sc.) degree in electrical engineering (cum laude) from Eindhoven University of Technology in December 1986. His thesis addressed the spatial distribution of packet traffic in a mobile ALOHA network. During his military service (January 1987–April 1988), he was with The Netherlands Organisation for Applied Scientific Research, Physics and Electronics Laboratory (F.E.L.-T.N.O.), The Hague, where he was involved in research on UHF propagation and frequency assignment for mobile and transportable radio networks. He joined Delft University of Technology in May 1988 as "universitair docent" (Assistant Professor) in the Telecommunications and Traffic-Control Systems Group. Currently, he is in the Department of Electrical Engineering and Computer Sciences (EECS) at the University of California at Berkeley. During his academic studies; he worked in local radio stations in Geleen; Bilzen, Belgium; and Delft; and with "Regionale Omroep Zuid" (currently, "Omroep Limburg") in Maastricht. He is the author of a number of magazine articles on technical aspects of radio broadcasting.

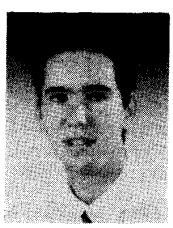

Aart J. 'T Jong was born in Sliedrecht, The Netherlands, on March 26, 1969. He attended Atheneum β at "De Lage Waard" Papendrecht. He received the Ir. (M.Sc.) degree in electrical engineering from Delft University of Technology, The Netherlands, in June 1992.

During his study he joined the Telecommunications and Traffic-Control Systems Group at Delft University of Technology in 1990, where he became involved in the research on mobile cellular radio communications. His thesis dealt with the performance of personal communication systems. Since July 1992, he has been serving the Dutch Army to fulfill his military service requirement in The Netherlands. His research interests are in the field of mobile radio communications.

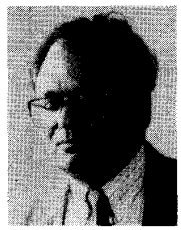

Ramjee Prasad (M'88–SM'90) was born in Babhnaur (Gaya), Bihar, India, on July 1, 1946. He received the B.Sc. (Eng.) from Bihar Institute of Technology, Sindri, India, and the M.Sc. (Eng.) and the Ph.D. degrees from Birla Institute of Technology (BIT), Ranchi, India, in 1968, 1970, and 1979, respectively.

He joined BIT as a Senior Research Fellow in 1970 and became Associate Professor in 1980. During 1983–1988 he was with the University of Dar es Salaam (UDSM), Tanzania, where he became Professor in Telecommunications at the Department of Electrical Engineering in 1986. Since February 1988, he has been with the Telecommunications and Traffic-Control Systems Group, Delft University of Technology, The Netherlands, where he is actively involved in the area of mobile and indoor radio communications. While he was with BIT, he supervised many research projects in the area of microwave and plasma engineering. AT UDSM he was responsible for the collaborative project "Satellite Communications for Rural Zones" with Eindhoven University of Technology, The Netherlands. He has published over 150 technical papers. His current research interest lies in packet communications, adaptive equalizers, spread-spectrum CDMA systems, and multimedia communications.

Dr. Prasad has served as a member of advisory and program committees of several IEEE international conferences. He has also presented tutorials on mobile and indoor radio communications at various universities, technical institutions, and IEEE conferences. He is also a member of working group of European co-operation in the field of scientific and technical research (COST-231) project dealing with "Evolution of Land Mobile Radio (including personal) Communications" as expert for The Netherlands. Prof. Prasad is listed in the *U.S. Who's Who in the World.* He is Organizer and Interim Chairman of IEEE Vehicular Technology/Communications Society Joint Chapter, Benelux Section. He is an Associate Technical Editor of IEEE COMMUNICATIONS MAGAZINE. He is a Fellow of the IEE, U.K., and the Institution of Electronics & Telecommunication Engineers and a member of the New York Academy of Sciences.